Asociación Argentina
de Mecánica Computacional

Mecánica Computacional Vol XXIX, págs. 1649-1672 (artículo completo)
Eduardo Dvorkin, Marcela Goldschmit, Mario Storti (Eds.)
Buenos Aires, Argentina, 15-18 Noviembre 2010

AN EULERIAN FINITE ELEMENT WITH FINITE ROTATIONS FOR THIN-WALLED COMPOSITE BEAMS

C. Martín Saravia[a,b], Sebastián P. Machado[a,b] and Víctor H. Cortínez[a,b]

[a] *Grupo Análisis de Sistemas Mecánicos, Centro de Investigación en Mecánica Teórica y Aplicada, Universidad Tecnológica Nacional, Facultad Regional Bahía Blanca, 11 de Abril 461, 8000 Bahía Blanca, Argentina.*

[b] *CONICET*

Key words: Geometrically exact beams; Anisotropic; Nonlinear Finite Elements

Abstract. An Eulerian beam finite element for composite thin-walled beams considering arbitrary displacements and rotations is presented. As a distinct feature, the virtual work equations are written as a function of generalized strain components, which are parametrized in terms of the director field and its derivatives. The generalized strains and forces are obtained via a transformation that maps generalized components into physical components. Finite rotations are parametrized with the incremental rotation tensor and an iterative multiplicative update of the director field is proposed. The formulation of the constitutive equation of the composite material is aided by a curvilinear transformation of the strain tensor. The proposed formulation is also valid for both isotropic and anisotropic beams. Different tests are performed to validate de formulation.

1 INTRODUCTION

The use of composite thin walled beams in different areas of engineering has been increasing since mathematical methods for describing complex structural behaviors started to be developed. With the use of the finite element method different formulations for beams have been reported, but some subjects, such as the inclusion of anisotropic materials in displacement based geometrically exact beam theories, have not been treated yet. As a matter of fact, the development of a displacement based finite element formulation for geometrically exact thin-walled beams made of composite materials is still not reported in the literature.

A geometrically exact beam theory must provide exact relations between the configuration and strains, in a fully consistent manner with the virtual work principle and regardless of the magnitude of the kinematic variables chosen to parametrize the configuration. It is well known that the treatment of finite rotations constitutes the main difficulty of a geometrically exact nonlinear formulation. In this work, we choose a set of variables to represent *exactly* the kinematic behavior of the thin-walled beam and develop a method to derive the relationships between the strains and the configuration.

Several authors have studied geometrically exact beam finite element formulations after the works of Reissner (1972) and Antman (1976) appeared in the early 70's. Also, an extensive and detailed study of finite rotations was made by Argyris (1982). Besides describing key aspects of spatial and material rotations he also clarifies the so called semitangential rotations, for which commutativity holds.

Updated and Total Lagrangian formulations valid for large displacements and based on a degenerate continuum concept were presented by Bathe and Bolourchi (1979). Simo (1985) and Simo and Vu-Quoc (1986) developed a 3D geometrically exact formulation for isotropic hyperelastic beams. They used the Reissner relationships between the variation of the rotation tensor and the infinitesimal rotations to derive the strain-configuration relations, maintaining the geometric exactness of the theory. Simo (1985) parametrized the finite rotations with the rotation tensor, aided by the quaternion algebra to enhance the computational efficiency of the algorithm. He proposed a multiplicative update procedure for the rotational changes, obtaining a non-symmetric tangent stiffness.

In contrast, Cardona and Geradin (1988) presented a different alternative of parametrization, using the total rotational pseudo-vector to update the 3D rotations on the basis of the initial configuration. They also proposed an alternative approach, updating the configuration on the basis of the last converged configuration (in what could be understood as an updated Lagrangian approach). This additive treatment of the rotational degrees of freedom gives rise to a symmetrical tangent stiffness. An isotropic hyperelastic constitutive law was assumed.

An extension of Simo's formulation to curved beams was presented by Ibrahimbegovic (1995). He extended the formulation to arbitrary curved space beams maintaining some key aspects of Simo formulation but using hierarchical interpolation. He also proposed an incremental rotation vector formulation (Ibrahimbegovic, 1997) to solve the nonlinear dynamics of space beams.

The use of the Green-Lagrange strain measures in a geometrically exact finite element formulation for 3D beams seems to have been first introduced first by Gruttmann (1998).

An extensive and detailed review of several aspects of existent geometrical nonlinear finite element formulations of beams was presented by Crisfield (1997), describing essential aspects of geometrical nonlinear beam theories and focusing the attention in the treatment of finite rotations.

Betsch and Steinmann (2002), Armero and Romero (2001) and Romero and Armero (2002) further contributed to the subject presenting frame-invariant formulations for geometrically exact beams using the director field to parametrize the equations of motion.

All the aforementioned formulations deal with solid cross section beams. As a consequence, the extension of these formulations to thin-walled beams is not natural. The advantage of thin-walled beam formulations is that the inclusion of anisotropic materials is natural.

The inclusion of anisotropic materials to thin-walled and also solid beam finite element formulations was studied by Hodges. He developed a geometrically-exact, fully intrinsic theory for dynamics of curved and twisted composite beams, having neither displacement nor rotation variables appearing in the formulation (Hodges et al., 2009).

Extensive work on analytical methods for solving geometrically nonlinear problems of composite thin-walled beams was done by Librescu (2006). He used different analytical approaches to treat composite beams undergoing moderate rotations, treating rotation variables in a vectorial fashion. Piovan and Cortínez (2007) and Machado (2005) presented a formulation for composite beams undergoing moderate rotations. Both formulations rely on an assumed displacement field, considering “vectorial” rotation variables up to a certain order.

This work presents an implementation of the classical thin-walled beam theory in a geometrically exact (configuration based) Eulerian finite element formulation. The rotation variables are treated exactly, and thus the varied configuration is obtained considering that the rotation variables belong to a SO(3) manifold.

This formulation is based on an assumed displacement field that, as said before, describes the kinematic behavior of the beam regardless of the magnitude of displacements and rotations. Following the classical procedure of the theory of thin walled beams, we develop the expressions for the Green-Lagrange (GL) strains and then transform these strains to a curvilinear coordinate system. To ease that process, we first express the GL strains in terms of generalized strains by the introduction of a linear transformation. These generalized strains are written in terms of the director vectors, its derivatives and the derivatives of the position vector of the center of reduction (the pole). This leads to a remarkable simple expression for the curvilinear strains.

Extracting from the GL strains the functions that describe the cross section shape we can write the virtual work only in terms of generalized strains and generalized beam forces. The equations of motion are thus parametrized in terms of the director field and their variations.

The parametrization of finite rotations is done using spatial spin variables, obtaining a natural relationship between the director field and the configuration. This spins variables are then interpolated using linear interpolation and the rotation tensor is calculated and updated for each iteration only at the integration points. The update of the derivatives of the director field is performed iteratively on the basis of the last iterative configuration, eliminating the necessity of calculating the incremental rotation tensor.

2 KINEMATICS

2.1 Generalities

Consider two states of the beam, an undeformed reference state, denoted by $\boldsymbol{\mathcal{B}}_{\mathbf{0}}$, and a deformed state, denoted by $\boldsymbol{\mathcal{B}}$, as shown in Fig. 1. Being $\boldsymbol{a}_i$ a spatial frame of reference, we define a reference frame $\boldsymbol{E}_i$ and a current frame $\boldsymbol{e}_i$ (both frames being orthonormal).

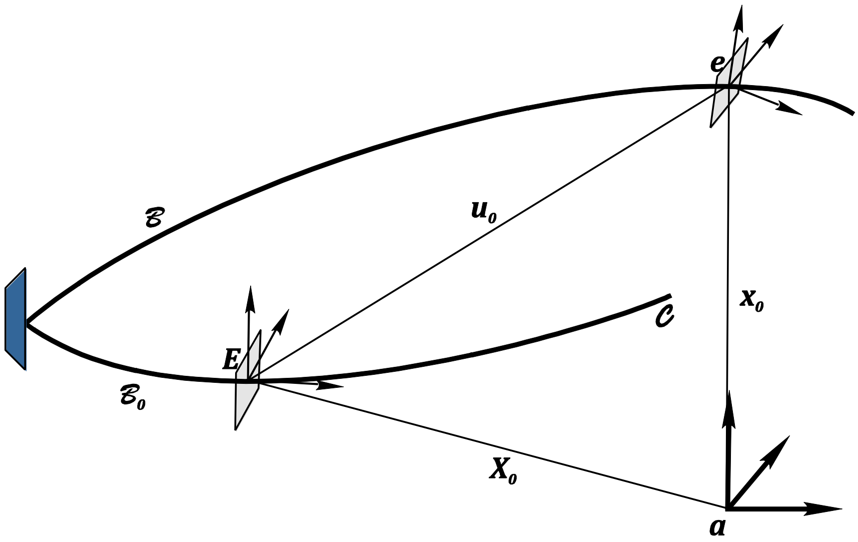

Figure 1. Kinematic description

The displacement of any point in the deformed beam measured with respect to the undeformed reference state can be expressed in the global coordinate system $\boldsymbol{a}_i$ in terms of a vector $\boldsymbol{u} = (u_1, u_2, u_3)$.

The current frame $\boldsymbol{e_i}$ is a function of a running length coordinate along the reference line of the beam, denoted as x, and is fixed to the beam cross-section. For convenience, we choose the reference curve $\mathcal{C}$ to be the locus of cross-sectional inertia centroids. The origin of $\boldsymbol{e}_i$ is located on the reference line of the beam and is called: *pole*. The cross-section of the beam is arbitrary and initially normal to the reference line of the beam.

The relations between the orthonormal frames are given by the linear transformations:

$$\boldsymbol{E}_i = \boldsymbol{\Lambda_0}(x)\boldsymbol{a}_i, \qquad \boldsymbol{e}_i = \boldsymbol{\Lambda}(x)\boldsymbol{E}_i, \tag{1}$$

where $\boldsymbol{\Lambda}_0(x)$ and $\boldsymbol{\Lambda}(x)$ are two-point tensor fields $\in \mathrm{SO}(3)$; the special orthogonal (Lie) group. Thus, it's satisfied that:

$$\boldsymbol{\Lambda_0}^{\boldsymbol{T}}\boldsymbol{\Lambda_0} = \mathbf{1}, \qquad \boldsymbol{\Lambda}^{\boldsymbol{T}}\boldsymbol{\Lambda} = \mathbf{1}. \tag{2}$$

Throughout this work we will consider that the beam element is straight, so we set $\boldsymbol{\Lambda_0} = \mathbf{1}$. Considering the relations (1), we express the position vectors of a point in the beam in the undeformed and deformed configuration respectively as:

$$\boldsymbol{X}(x, \xi_2, \xi_3) = \boldsymbol{X}_0(x) + \sum_2^3 \xi_i\, \boldsymbol{E}_i, \qquad \boldsymbol{x}(x, \xi_2, \xi_3, t) = \boldsymbol{x}_0(x, t) + \sum_2^3 \xi_i\, \boldsymbol{e}_i. \tag{3}$$

where in both equations the first term stands for the position of the pole and the second term stands for the position a point in the cross section relative to the pole. Note that, x is the running length coordinate and ξ_2 and ξ_3 are cross section coordinates.

Also, it is possible to express the displacement field as:

$$\boldsymbol{u}(x, \xi_2, \xi_3, t) = \boldsymbol{x} - \boldsymbol{X} = \boldsymbol{u}_0(x, t) + (\boldsymbol{\Lambda} - \mathbf{I}) \sum_2^3 \xi_i\, \boldsymbol{E}_i, \tag{4}$$

where $\boldsymbol{u}_0$ represents the displacement of the kinematic center of reduction, i.e. the pole. Note that t is the pseudo-time variable. The set of kinematic variables is defined by three displacements and three spins as:

$$\mathcal{V} := \{\boldsymbol{\phi} = [\boldsymbol{u}, \boldsymbol{w}]^T : [0, \ell] \rightarrow R^3\},$$
$$[\boldsymbol{u}, \boldsymbol{w}]^{\boldsymbol{T}} = [u_1, u_2, u_3, w_1, w_2, w_3]^{\boldsymbol{T}}. \tag{5}$$

2.2 Parametrization of Finite Rotations

According to the kinematic description presented previously, the beam configuration space consists on a linear space of three-dimensional vectors $\boldsymbol{u}_0$ and a nonlinear manifold of transformations $\boldsymbol{\Lambda}$ (a special orthogonal Lie Group SO(3)). This transformation is described mathematically via the exponential map as:

$$\boldsymbol{\Lambda}(\boldsymbol{\theta}) = \cos\theta\, \boldsymbol{I} + \frac{\sin\theta}{\theta}\boldsymbol{\Theta} + \frac{1-\cos\theta}{\theta^2}\boldsymbol{\theta}\otimes\boldsymbol{\theta}, \tag{6}$$

where $\boldsymbol{\theta}$ is the so-called rotation vector, θ its modulus and $\boldsymbol{\Theta}$ is its skew symmetric matrix.

In this work we parametrize finite rotations with the rotation tensor, using spins as rotation variables. The update of the directors is performed in a multiplicative way at each iteration. With this implementation the total rotation tensor from the last converged configuration to the current configuration is not needed, leading to a very simple and effective algorithm.

It is well known the fact that this parametrization of finite rotations leads to a nonsymmetrical tangent stiffness matrix for non-equilibrium configuration. This is caused by the use of non-additive (even in the limit) spin variables, see e.g. (Crisfield, 1997)

3 STRAIN AND STRESS FIELDS

3.1 The Strain Tensor

In contrast with most existing formulations for thin-walled beams (see e.g. (Librescu, 2006, Machado and Cortínez, 2005)) we express the GL strain tensor in terms of reference and current position derivatives. We operate in a conventional way by injecting the tangent vectors $\boldsymbol{G_i} = \boldsymbol{X}_{,i}$ and $\boldsymbol{g_i} = \boldsymbol{x}_{,i}$ into the GL strain tensor:

$$\boldsymbol{\varepsilon_{GL}} = \boldsymbol{\varepsilon}_{ij}\boldsymbol{G}^i\otimes\boldsymbol{G}^j. \tag{7}$$

The components with respect to the dual basis system $\boldsymbol{G}^i$ defined by $\boldsymbol{G}_i \cdot \boldsymbol{G}^i = \delta_i^j$ (see e.g. (Bonet, 1997)) are:

$$\boldsymbol{E}_{GL} = \tfrac{\boldsymbol{1}}{\boldsymbol{2}}\left(\boldsymbol{x}_{,i} \cdot \boldsymbol{x}_{,j} - \boldsymbol{X}_{,i} \cdot \boldsymbol{X}_{,j}\right). \tag{8}$$

According to the kinematic hypotheses, the non-vanishing components of the GL strain tensor are only three, in vector notation:

$$\boldsymbol{E}_{GL} = [E_{11} \quad 2E_{12} \quad 2E_{13}]^T, \tag{9}$$

where:

$$E_{11} = \frac{1}{2}\left(\boldsymbol{x}_0'^{\,2} - \boldsymbol{X}_0'^{\,2}\right) + \xi_2\left(\boldsymbol{x}_0' \cdot \boldsymbol{e}_3' - \boldsymbol{X}_0' \cdot \boldsymbol{E}_3'\right) + \xi_3\left(\boldsymbol{x}_0' \cdot \boldsymbol{e}_2' - \boldsymbol{X}_0' \cdot \boldsymbol{E}_2'\right)$$
$$+\frac{1}{2}\xi_2^2\left(\boldsymbol{e}_2'^{\,2} - \boldsymbol{E}_2'^{\,2}\right) + \frac{1}{2}\xi_3^2\left(\boldsymbol{e}_3'^{\,2} - \boldsymbol{E}_3'^{\,2}\right) + \xi_2\xi_3\left(\boldsymbol{e}_2' \cdot \boldsymbol{e}_3' - \boldsymbol{E}_2' \cdot \boldsymbol{E}_3'\right), \tag{10}$$

$$E_{12} = \frac{1}{2}\left[\boldsymbol{x}_0' \cdot \boldsymbol{e}_2 - \boldsymbol{X}_0' \cdot \boldsymbol{E}_2 - \xi_3\left(\boldsymbol{e}_3' \cdot \boldsymbol{e}_2 - \boldsymbol{E}_3' \cdot \boldsymbol{E}_2\right)\right],$$

$$E_{13} = \frac{1}{2}\left[\boldsymbol{x}_0' \cdot \boldsymbol{e}_3 - \boldsymbol{X}_0' \cdot \boldsymbol{E}_3 + \xi_2\left(\boldsymbol{e}_2' \cdot \boldsymbol{e}_3 - \boldsymbol{E}_2' \cdot \boldsymbol{E}_3\right)\right].$$

In order to ease the derivation of the thin-walled beam strains we introduce a new entity; the *generalized strain vector* $\boldsymbol{\varepsilon}$. The generalized strain vector is a vector that properly transformed gives the GL strain vector. This transformation actually "separates" from the GL strain vector the variables related to the location of a point in the cross section (i.e. ξ_i). Therefore, the mentioned transformation gives:

$$\boldsymbol{E}_{GL} = \boldsymbol{D}\, \boldsymbol{\varepsilon}, \tag{11}$$

where the transformation matrix is:

$$\boldsymbol{D} = \begin{bmatrix} 1 & \xi_3 & \xi_2 & 0 & 0 & 0 & \frac{1}{2}{\xi_2}^2 & \frac{1}{2}{\xi_3}^2 & \xi_2\xi_3 \\ 0 & 0 & 0 & 1 & 0 & -\xi_3 & 0 & 0 & 0 \\ 0 & 0 & 0 & 0 & 1 & \xi_2 & 0 & 0 & 0 \end{bmatrix}. \tag{12}$$

And the generalized strain vector is:

$$\boldsymbol{\varepsilon} = \begin{bmatrix} \epsilon \\ \kappa_2 \\ \kappa_3 \\ \gamma_2 \\ \gamma_3 \\ \kappa_1 \\ \chi_2 \\ \chi_3 \\ \chi_{23} \end{bmatrix} = \begin{bmatrix} \frac{1}{2}\left(\boldsymbol{x}_0' \cdot \boldsymbol{x}_0' - \boldsymbol{X}_0' \cdot \boldsymbol{X}_0'\right) \\ \boldsymbol{x}_0' \cdot \boldsymbol{e}_3' - \boldsymbol{X}_0' \cdot \boldsymbol{E}_3' \\ \boldsymbol{x}_0' \cdot \boldsymbol{e}_2' - \boldsymbol{X}_0' \cdot \boldsymbol{E}_2' \\ \boldsymbol{x}_0' \cdot \boldsymbol{e}_2 - \boldsymbol{X}_0' \cdot \boldsymbol{E}_2 \\ \boldsymbol{x}_0' \cdot \boldsymbol{e}_3 - \boldsymbol{X}_0' \cdot \boldsymbol{E}_3 \\ \boldsymbol{e}_2' \cdot \boldsymbol{e}_3 - \boldsymbol{E}_2' \cdot \boldsymbol{E}_3 \\ \boldsymbol{e}_2' \cdot \boldsymbol{e}_2' - \boldsymbol{E}_2' \cdot \boldsymbol{E}_2' \\ \boldsymbol{e}_3' \cdot \boldsymbol{e}_3' - \boldsymbol{E}_3' \cdot \boldsymbol{E}_3' \\ \boldsymbol{e}_2' \cdot \boldsymbol{e}_3' - \boldsymbol{E}_2' \cdot \boldsymbol{E}_3' \end{bmatrix}. \tag{13}$$

The derivation of strains and stresses measures for thin-walled beams is aimed by the introduction of an orthogonal curvilinear coordinate system (x, n, s), see Fig. 2. The cross-section shape will be defined in this coordinate system by functions $\xi_i(n, s)$. The coordinate s is measured along the tangent to the middle line of the cross section, in clockwise direction and with origin conveniently chosen. Also, the thickness coordinate $n(-e/2 \leq e/2)$ is perpendicular to s and with origin in the middle line contour.

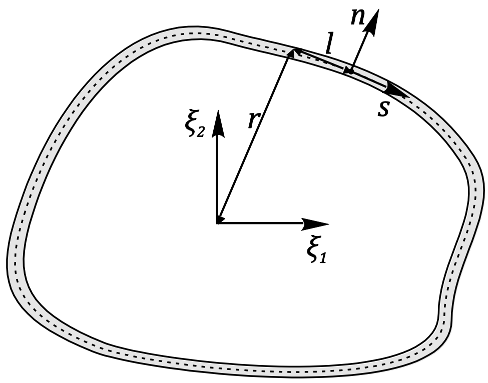

Figure 2 – Curvilinear Transformation Schematic

In order to represent the GL strains in this curvilinear coordinate system we make use of the curvilinear transformation tensor:

$$\boldsymbol{P} = \begin{bmatrix} 1 & 0 & 0 \\ 0 & \dfrac{d\bar{\xi}_2}{ds} & \dfrac{d\bar{\xi}_3}{ds} \\ 0 & -\dfrac{d\bar{\xi}_3}{ds} & \dfrac{d\bar{\xi}_2}{ds} \end{bmatrix}. \tag{14}$$

where the functions $\bar{\xi}_i$ describe the mid-contour of the cross section.

Hence, the GL strain vector in the curvilinear coordinate system, $\widehat{\boldsymbol{E}}_{GL}$, is obtained by transforming the rectangular GL strains as:

$$\widehat{\boldsymbol{E}}_{GL} = [E_{xx} \quad 2E_{xs} \quad 2E_{xn}]^T = \boldsymbol{P}\,\boldsymbol{E}_{GL}, \tag{15}$$

$$\widehat{\boldsymbol{E}}_{GL} = \boldsymbol{P}\,\boldsymbol{D}\,\boldsymbol{\varepsilon} = \widehat{\boldsymbol{D}}\,\boldsymbol{\varepsilon}. \tag{16}$$

Recalling (12) and (13), it's found that the GL strain vector in curvilinear coordinates has a remarkably simple closed expression:

$$\widehat{\boldsymbol{E}}_{GL} = \begin{bmatrix} \epsilon + \xi_2\kappa_3 + \xi_3\kappa_2 + \frac{1}{2}{\xi_2}^2\chi_2 + \frac{1}{2}{\xi_3}^2\chi_3 + \xi_2\xi_3\chi_{23} \\ \bar{\xi}_2'\gamma_2 + \bar{\xi}_3'\gamma_3 + \left(\xi_2\bar{\xi}_3' - \xi_3\bar{\xi}_2'\right)\kappa_1 \\ -\bar{\xi}_3'\gamma_2 + \bar{\xi}_2'\gamma_3 + \left(\xi_2\bar{\xi}_2' + \xi_3\bar{\xi}_3'\right)\kappa_1 \end{bmatrix}, \tag{17}$$

where the prime symbol has been used to denote derivation with respect to the *s* coordinate.

Proceeding in a similar way as done in (11), we separate from $\widehat{\boldsymbol{E}}_{GL}$ the quantities related to the middle-line coordinate s and the quantities related to the thickness coordinate n. Before, we can refer to Fig. 2 (see also (Machado and Cortínez, 2005)) to easily verify that the location of a point anywhere in the cross-section can be expressed as:

$$\xi_2(n,s) = \bar{\xi}_2(s) - n\frac{d\bar{\xi}_3}{ds}, \qquad \xi_3(n,s) = \bar{\xi}_3(s) + n\frac{d\bar{\xi}_2}{ds}, \tag{18}$$

where ξ_i locates a point anywhere in the cross section and $\bar{\xi}_i$ locates the points lying in the middle-line contour. Introducing (18) into the matrix $\widehat{\boldsymbol{D}}$, defined in (16), we can obtain a cross sectional matrix $\widehat{\boldsymbol{D}}$ that is a function only of the midsurface coordinates $\bar{\xi}_i$. This form of $\widehat{\boldsymbol{D}}$ will be used hereafter. The expression of this matrix is given in Appendix A.

As it will be clarified in the next section, we will use five independent curvilinear strain measures (collected in the vector $\boldsymbol{\epsilon}_s$) to describe the strain state of the thin-walled beam, or more exactly; a laminate (see e.g. (Barbero, 2008, Jones, 1999)). Thus, the strain state of the beam will be described by:

$$\boldsymbol{\epsilon}_s = [\varepsilon_{xx} \quad \gamma_{xs} \quad \gamma_{xn} \quad \varkappa_{xx} \quad \varkappa_{xs}]^T. \tag{19}$$

Pursuing the mentioned objective of describing the strain state of the beam in terms of the generalized strain vector, we propose a matrix $\boldsymbol{\mathcal{T}}$ to establish the relationship between the GL curvilinear strains and the generalized strains as:

$$\boldsymbol{\epsilon}_s = \boldsymbol{\mathcal{T}}\,\boldsymbol{\varepsilon}. \tag{20}$$

Substituting (18) into (17), we obtain:

$$\boldsymbol{\mathcal{T}}(s) = \begin{bmatrix} 1 & \bar{\xi}_3 & \bar{\xi}_2 & 0 & 0 & 0 & 0 & 0 & \frac{1}{2}\bar{\xi}_2^{\ 2} & \frac{1}{2}\bar{\xi}_3^{\ 2} & \bar{\xi}_2\bar{\xi}_3 \\ 0 & 0 & 0 & \bar{\xi}_2' & \bar{\xi}_3' & \bar{\xi}_2\bar{\xi}_3' - \bar{\xi}_3\bar{\xi}_2' & \bar{\xi}_2\bar{\xi}_2' & \bar{\xi}_3\bar{\xi}_3' & 0 & 0 & 0 \\ 0 & 0 & 0 & -\bar{\xi}_3' & \bar{\xi}_2' & \bar{\xi}_2\bar{\xi}_2' + \bar{\xi}_3\bar{\xi}_3' & -\bar{\xi}_2\bar{\xi}_3' & \bar{\xi}_3\bar{\xi}_2' & 0 & 0 & 0 \\ 0 & \bar{\xi}_2' & -\bar{\xi}_3' & 0 & 0 & 0 & 0 & 0 & -\bar{\xi}_2\bar{\xi}_3' & \bar{\xi}_3\bar{\xi}_2' & \left(\bar{\xi}_2\bar{\xi}_2' - \bar{\xi}_3\bar{\xi}_3'\right) \\ 0 & 0 & 0 & 0 & 0 & -\left(\bar{\xi}_2'^{\ 2} + \bar{\xi}_3'^{\ 2}\right) & -\bar{\xi}_2'\bar{\xi}_3' & \bar{\xi}_2'\bar{\xi}_3' & 0 & 0 & 0 \end{bmatrix}, \quad (21)$$

Where we have neglected the terms in n^2.

3.2 Composite Mechanics - Constitutive Relations

According to the theory of thin-walled composite laminates (Barbero, 2008), we can express:

$$\begin{bmatrix} N_{xx} \\ N_{xs} \\ N_{xn} \\ M_{xx} \\ M_{xs} \end{bmatrix} = \begin{bmatrix} \bar{A}_{11} & \bar{A}_{16} & 0 & \bar{B}_{11} & \bar{B}_{16} \\ \bar{A}_{16} & \bar{A}_{66} & 0 & \bar{B}_{16} & \bar{B}_{66} \\ 0 & 0 & \bar{A}_{55}^{H} & 0 & 0 \\ \bar{B}_{11} & \bar{B}_{16} & 0 & \bar{D}_{11} & \bar{D}_{16} \\ \bar{B}_{16} & \bar{B}_{66} & 0 & \bar{D}_{16} & \bar{D}_{66} \end{bmatrix} \begin{bmatrix} \varepsilon_{xx} \\ \gamma_{xs} \\ \gamma_{xn} \\ \varkappa_{xx} \\ \varkappa_{xs} \end{bmatrix}, \quad (22)$$

where $\bar{A}_{\mathrm{ij}}$ are components of the laminate reduced in-plane stiffness matrix, $\bar{B}_{\mathrm{ij}}$ are components of the reduced bending-extension coupling matrix, $\bar{D}_{\mathrm{ij}}$ are components of the reduced bending stiffness matrix and $\bar{A}_{55}^{H}$ is the component of the reduced transverse shear stiffness matrix.

We can express the above relation in matrix form as:

$$\boldsymbol{N}_s = \boldsymbol{C}\,\boldsymbol{\epsilon}_s, \quad (23)$$

where $\boldsymbol{C}$ is the composite shell constitutive matrix and $\boldsymbol{\epsilon}_s$ is the curvilinear shell strain vector defined in (20).

Now, it is possible to express the shell forces as a function of the generalized strains. Replacing (20) into (23) we obtain;

$$\boldsymbol{N}_s = \boldsymbol{C}\,\boldsymbol{\mathcal{T}}\,\boldsymbol{\varepsilon}. \quad (24)$$

Now, we transform the shell forces in (24) back to the "generalized space" by using the double transformation matrix $\boldsymbol{\mathcal{T}}$**.** Thus, we obtain a new entity, a sort of transformed back shell strain:

$$\boldsymbol{N}_s^G = \boldsymbol{\mathcal{T}}^T \boldsymbol{N}_s = \boldsymbol{\mathcal{T}}^T \boldsymbol{C}\,\boldsymbol{\mathcal{T}}\,\boldsymbol{\varepsilon}. \quad (25)$$

Although at first glance this stress could seem contrived, it can be observed that it is a vector of generalized shell stresses defined in the global coordinate system. Since $\boldsymbol{N}_s^G$ is a function of the cross section contour, integration over the contour gives the vector of generalized beam forces, work conjugate with the generalized strains, as:

$$\boldsymbol{S}(x) = \int_S \boldsymbol{N}_s^G ds = \left(\int_S \boldsymbol{\mathcal{T}}^T \boldsymbol{C}\,\boldsymbol{\mathcal{T}}\,ds\right)\boldsymbol{\varepsilon}(x), \quad (26)$$

$$\boldsymbol{S}(x) = \boldsymbol{\mathcal{D}}\,\boldsymbol{\varepsilon}(x). \quad (27)$$

Note that since the generalized strain vector $\boldsymbol{\varepsilon}$ is not a function of the curvilinear coordinate s, see (13), it was taken out of the integral over the contour. Also, the matrix $\boldsymbol{\mathcal{D}}$ was defined as:

$$\boldsymbol{\mathcal{D}} = \int_S \boldsymbol{\mathcal{T}}^T \boldsymbol{C}\, \boldsymbol{\mathcal{T}}\, ds. \tag{28}$$

The matrix $\boldsymbol{\mathcal{D}}$ contains functions $\bar{\xi}_i$ that define the cross section mid-contour and also all the necessary material constants. It's of crucial importance the correct evaluation and formulation of $\boldsymbol{\mathcal{D}}$ since it contains not only all geometrical couplings but also all material couplings.

The last derivations complete the formulation of the constitutive relations of the thin-walled beam theory. In contrast with most existing thin-walled beam formulations, the beam forces were not defined but deduced from the shell stresses (or forces) expression.

4 VARIATIONAL FORMULATION

The expression for the director variations depends on the perturbed rotation tensor, which must be found as a function of the rotation variables chosen to parametrize the finite rotations. Once the set of kinematically admissible variations is obtained, the generalized virtual strains can be obtained, so the virtual work of the internal and external forces can be derived. Therefore, the objective of this section is to express the virtual work principle as a function of the generalized virtual strain vector and its work conjugate beam forces vector.

The weak form of equilibrium of a three dimensional body $\boldsymbol{\mathcal{B}}$ is given by:

$$G(\boldsymbol{\phi}, \delta\boldsymbol{\phi}) = \int_{\mathcal{B}} \boldsymbol{\sigma} \cdot \delta\boldsymbol{\epsilon}\, dV - \int_{\mathcal{B}} \boldsymbol{\rho_0 b} \cdot \delta\boldsymbol{\phi}\, dV - \int_{\partial\mathcal{B}} (\boldsymbol{p} \cdot \delta\boldsymbol{u} + \boldsymbol{m} \cdot \delta\boldsymbol{w})\, d\Omega, \tag{29}$$

where $\boldsymbol{b}$, $\boldsymbol{p}$ and $\boldsymbol{m}$ are: body forces, prescribed external forces and prescribed external moments per unit length respectively (Washizu, 1968, Zienkiewicz, 2000). $\boldsymbol{\epsilon}$ is the GL strain tensor, work conjugate to the Second Piola-Kirchhoff stress tensor $\boldsymbol{\sigma}$. Where $\boldsymbol{\sigma}$ could be defined in either a rectangular or a curvilinear coordinate system, such a distinction is, at least here, unnecessary.

4.1 Admissible variations and perturbed rotation field

Now it is necessary to define the space of kinematically admissible variations in terms of the independent kinematic variables. To obtain the generalized strains variations we need to find first the admissible variation of the basis vectors. Remembering that we set $\boldsymbol{\Lambda_0} = \boldsymbol{I}$ and recalling (1), we can write:

$$\delta\boldsymbol{e}_i = \delta(\boldsymbol{\Lambda}(\mathrm{s})\boldsymbol{E}_i) = \delta\boldsymbol{\Lambda}(x)\boldsymbol{E}_i. \tag{30}$$

The admissible variation of the rotation tensor (Lie variation) can be obtained introducing an infinitesimal virtual rotation superposed onto the existing finite rotation. This virtual rotation lies in the tangent space at $\boldsymbol{\Lambda}$ (spatial virtual rotation), or in the tangent space at $\mathbf{I}$ (material virtual rotation), and is represented by a skew symmetric matrix $\delta\boldsymbol{W}$, or $\delta\boldsymbol{\Psi}$.

These variables will be called: "*spins*" (Crisfield, 1997). The perturbed rotation tensor is constructed by exponentiating the spatial spin as:

$$\boldsymbol{\Lambda}_\epsilon = exp(\epsilon\, \delta\boldsymbol{W})\boldsymbol{\Lambda}. \tag{31}$$

Now, being $\mathbf{\Lambda}$ a two point tensor that takes vectors from the tangent space in the initial configuration to the tangent space in the current configuration, we can use it to relate spatial and material spins respectively as:

$$\delta\boldsymbol{\Psi} = \boldsymbol{\Lambda}^T\,\delta\boldsymbol{W}\,\boldsymbol{\Lambda}, \qquad \delta\boldsymbol{W} = \boldsymbol{\Lambda}\,\delta\boldsymbol{\Psi}\,\boldsymbol{\Lambda}^T. \tag{32}$$

From which we can write the material version of the kinematically admissible perturbed finite rotation tensor as:

$$\boldsymbol{\Lambda}_\epsilon = \boldsymbol{\Lambda}\,exp(\epsilon\,\delta\boldsymbol{\Psi}). \tag{33}$$

Recalling (31) we can express the variation of the rotation tensor in terms of the spatial spin as:

$$\delta\mathbf{\Lambda} = \frac{d}{d\epsilon}[exp(\epsilon\,\delta\boldsymbol{W})\mathbf{\Lambda}]|_{\epsilon=0} = \delta\boldsymbol{W}\mathbf{\Lambda}. \tag{34}$$

Again, $\delta\boldsymbol{W}$ is a skew symmetric matrix such as:

$$\delta\boldsymbol{W}\boldsymbol{a} = \delta\boldsymbol{w}\times\boldsymbol{a}. \tag{35}$$

Therefore, we can rewrite (30) as:

$$\delta\boldsymbol{e}_i = \delta\boldsymbol{w}\times\boldsymbol{e}_i. \tag{36}$$

Considering the last relationship, the set of kinematically admissible variations is defined as:

$$\delta\mathcal{V} := \{\delta\boldsymbol{\phi} = [\delta\boldsymbol{u}, \delta\boldsymbol{w}]^T : [0,\ell] \to R^3 | \delta\boldsymbol{\phi} = 0 \text{ on } \mathcal{S}\}, \tag{37}$$

where $\mathcal{S}$ describes de boundaries with prescribed displacements and rotations.

Additionally, we can find the variation of the director's derivative as:

$$\delta\boldsymbol{e}_i' = \delta\boldsymbol{w}'\times\boldsymbol{e}_i + \delta\boldsymbol{w}\times\boldsymbol{e}_i'. \tag{38}$$

The variations of the directors and its derivatives are now used to obtain the generalized virtual strains variation. Considering that $\delta\boldsymbol{E_i} = 0$ and $\delta\boldsymbol{X}_0' = 0$, and performing the variation to (13) we obtain:

$$\delta\boldsymbol{\varepsilon} = \begin{bmatrix} \delta\epsilon \\ \delta\kappa_2 \\ \delta\kappa_3 \\ \delta\gamma_2 \\ \delta\gamma_3 \\ \delta\kappa_1 \\ \delta\chi_2 \\ \delta\chi_3 \\ \delta\chi_{23} \end{bmatrix} = \begin{bmatrix} \boldsymbol{x}_0'\cdot\delta\boldsymbol{u}' \\ \boldsymbol{e}_3'\cdot\delta\boldsymbol{u}' + \boldsymbol{x}_0'\cdot\delta\boldsymbol{e}_3' \\ \boldsymbol{e}_2'\cdot\delta\boldsymbol{u}' + \boldsymbol{x}_0'\cdot\delta\boldsymbol{e}_2' \\ \boldsymbol{e}_2\cdot\delta\boldsymbol{u}' + \boldsymbol{x}_0'\cdot\delta\boldsymbol{e}_2 \\ \boldsymbol{e}_3\cdot\delta\boldsymbol{u}' + \boldsymbol{x}_0'\cdot\delta\boldsymbol{e}_3 \\ \delta\boldsymbol{e}_2'\cdot\boldsymbol{e}_3 + \boldsymbol{e}_2'\cdot\delta\boldsymbol{e}_3 \\ 2(\delta\boldsymbol{e}_2'\cdot\boldsymbol{e}_2') \\ 2(\delta\boldsymbol{e}_3'\cdot\boldsymbol{e}_3') \\ \delta\boldsymbol{e}_2'\cdot\boldsymbol{e}_3' + \boldsymbol{e}_2'\cdot\delta\boldsymbol{e}_3' \end{bmatrix}. \tag{39}$$

Making use of (36) and (38) it is possible to rewrite (39) in the following form:

$$\delta\boldsymbol{\varepsilon} = \boldsymbol{H}(\boldsymbol{\Upsilon}\delta\boldsymbol{\phi}), \tag{40}$$

where $\boldsymbol{\Upsilon}$ is a matrix differential operator and $\boldsymbol{H}$ a matrix of director vectors such as:

$$
\boldsymbol{H} = \begin{bmatrix} \boldsymbol{x}_0' & \mathbf{0} & \mathbf{0} \\ \boldsymbol{e}_3' & \boldsymbol{e}_3' \times \boldsymbol{x}_0' & \boldsymbol{e}_3 \times \boldsymbol{x}_0' \\ \boldsymbol{e}_2' & \boldsymbol{e}_2' \times \boldsymbol{x}_0' & \boldsymbol{e}_2 \times \boldsymbol{x}_0' \\ \boldsymbol{e}_2 & \boldsymbol{e}_2 \times \boldsymbol{x}_0' & \mathbf{0} \\ \boldsymbol{e}_3 & \boldsymbol{e}_3 \times \boldsymbol{x}_0' & \mathbf{0} \\ \mathbf{0} & \mathbf{0} & \boldsymbol{e}_2 \times \boldsymbol{e}_3 \\ \mathbf{0} & \mathbf{0} & 2(\boldsymbol{e}_2 \times \boldsymbol{e}_2') \\ \mathbf{0} & \mathbf{0} & 2(\boldsymbol{e}_3 \times \boldsymbol{e}_3') \\ \mathbf{0} & \mathbf{0} & \boldsymbol{e}_3 \times \boldsymbol{e}_2' + \boldsymbol{e}_2 \times \boldsymbol{e}_3' \end{bmatrix}, \quad \boldsymbol{\Upsilon} = \begin{bmatrix} \frac{d}{dx}\mathbf{1} & \mathbf{0} \\ \mathbf{0} & \mathbf{1} \\ \mathbf{0} & \frac{d}{dx}\mathbf{1} \end{bmatrix}. \tag{41}
$$

It can be seen that the description of the exact kinematic behavior of the beam can be fully described using nine generalized quantities. This is in contrast with several approximated thin-walled beam formulations where more beam higher order forces appear and the exact kinematic behavior is still not represented (see e.g. (Librescu, 2006, Machado and Cortínez, 2005)).

The presented derivation of the virtual generalized strains in terms of the variations of the directors and its derivatives is independent of the parametrization of finite rotations. This is a very important fact since any known finite rotations algorithm could be used with the proposed formulation. Nonetheless, standard time stepping algorithms could be implemented without any additional modifications.

4.2 Internal Virtual Work

Having derived the expressions for the admissible variations of the basis vectors and strains we develop in this section the expressions for the internal virtual work of the beam. Recalling (29), the internal virtual work of a three dimensional body can be written in vector form as:

$$
G_{int}(\boldsymbol{\phi}, \delta\boldsymbol{\phi}) = \int_{\mathcal{B}_0} \delta\boldsymbol{\epsilon}^T \boldsymbol{\sigma}\, dV, \tag{42}
$$

which in the curvilinear coordinate system is:

$$
G_{int}(\boldsymbol{\phi}, \delta\boldsymbol{\phi}) = \int_{\ell} \int_{S} \int_{e} (\delta\boldsymbol{\epsilon}^T \boldsymbol{\sigma}\,)\; dn\, ds\, dx. \tag{43}
$$

We can now use the definition of the shell resultant forces to reduce the 3D formulation to a 2D formulation. Therefore, performing integration of (43) in the n direction we can write the internal virtual work in terms of shell quantities as:

$$
G_{int}(\boldsymbol{\phi}, \delta\boldsymbol{\phi}) = \int_{\ell} \int_{S} \delta\boldsymbol{\epsilon}_s^T\, \boldsymbol{N}_s\, ds\;\, dx. \tag{44}
$$

The reduction to a 1D formulation is aided by the deduction of 1D beam forces presented in (26). Transforming the virtual curvilinear shell strains into virtual generalized strains we can rewrite the last expression as:

$$
G_{int}(\boldsymbol{\phi}, \delta\boldsymbol{\phi}) = \int_{\ell} \delta\boldsymbol{\varepsilon}^T \left(\int_{S} \boldsymbol{\mathcal{T}}^T\, \boldsymbol{N}_s\, ds \right) dx \tag{45}
$$

In which the term in parentheses is the generalized beam forces vector (see (26)). Using (25) the beam forces vector can be expressed a slightly different form as:

$$\boldsymbol{S}(x) = \int_S \boldsymbol{\mathcal{T}}^T \boldsymbol{N}_s \, ds. \tag{46}$$

The explicit expression of the beam forces can be found in Appendix A.

Finally, it's possible write the 1D virtual work in terms of the generalized strains and the generalized beam forces as:

$$G_{int}(\boldsymbol{\phi}, \delta\boldsymbol{\phi}) = \int_\ell \delta\boldsymbol{\varepsilon}^T \boldsymbol{S} \, dx. \tag{47}$$

4.3 External Virtual Work

In this section we derive the expression of the external virtual work. In order to simplify this derivation we neglect the body forces. For this particular case, the external virtual work can be written as:

$$G_{ext}(\boldsymbol{\phi}, \delta\boldsymbol{\phi}) = \int_l (\boldsymbol{p} \cdot \delta\boldsymbol{u}_0 + \boldsymbol{m} \cdot \delta\boldsymbol{w}) \, dx, \tag{48}$$

where $\boldsymbol{p}$ is the external forces vector and $\boldsymbol{m}$ the external moments vector. As first noted by Ziegler (1968) moments about fixed axes are non-conservative. Consequently, the work is path-dependent if concentrated moments are applied (see (Ritto-Corrêa and Camotim, 2003) for a clarification of concepts).

4.4 Weak Form of Equilibrium

The variational equilibrium statement can now be presented in terms of generalized components of 1D forces and strains. Recalling (47) and (48) the virtual work of a composite beam is written in its one dimensional form as:

$$G(\boldsymbol{\phi}, \delta\boldsymbol{\phi}) = \int_\ell \delta\boldsymbol{\varepsilon}^T \boldsymbol{S} \, dx - \int_l (\boldsymbol{p} \cdot \delta\boldsymbol{u}_0 + \boldsymbol{m} \cdot \delta\boldsymbol{w}) \, dx. \tag{49}$$

Recalling (40) it's possible to re-write the last expression as:

$$G(\boldsymbol{\phi}, \delta\boldsymbol{\phi}) = \int_\ell [\boldsymbol{H}(\boldsymbol{\Upsilon}\delta\boldsymbol{\phi})]^T \boldsymbol{S} \, dx - \int_l (\boldsymbol{p} \cdot \delta\boldsymbol{u}_0 + \boldsymbol{m} \cdot \delta\boldsymbol{w}) \, dx. \tag{50}$$

Thus, the equilibrium of the geometrically nonlinear beam is available in its variational form.

5 LINEARIZATION OF THE WEAK FORM

The linearization of the variational equilibrium equations is obtained through the directional derivative and, assuming conservative loading, its application gives two tangent terms; the material and the geometric stiffness matrices.

Being $L[G(\boldsymbol{\phi}, \delta\boldsymbol{\phi})]$ the linear part of the functional $G(\phi, \delta\phi)$, we have:

$$L\left[G\left(\hat{\boldsymbol{\phi}}, \delta\boldsymbol{\phi}\right)\right] = G\left(\hat{\boldsymbol{\phi}}, \delta\boldsymbol{\phi}\right) + D\, G\left(\hat{\boldsymbol{\phi}}, \delta\boldsymbol{\phi}\right) \cdot \Delta\boldsymbol{\phi}, \tag{51}$$

where the first term $G\left(\hat{\boldsymbol{\phi}}, \delta\boldsymbol{\phi}\right)$ is the unbalanced force at the configuration $\hat{\boldsymbol{\phi}}$.

Using the definition of the Frechet differential and recalling (47) and (39), we obtain the tangent stiffness as:

$$D\,G_{int}(\boldsymbol{\phi},\delta\boldsymbol{\phi})\cdot\Delta\boldsymbol{\phi}=\int_{\ell}\left(\delta\boldsymbol{\varepsilon}^{T}\,\boldsymbol{\mathcal{D}}\,\Delta\boldsymbol{\varepsilon}+\Delta\delta\boldsymbol{\varepsilon}^{T}\,\boldsymbol{S}\right)dx, \tag{52}$$

where ℓ is the length of the undeformed beam. The integral of the first term gives raise to the material stiffness matrix and from the integral of the second term evolves the geometric stiffness matrix.

Recalling (40) the first term takes the form:

$$D_1G_{int}(\boldsymbol{\phi},\delta\boldsymbol{\phi})\cdot\Delta\boldsymbol{\phi}=\int_{\ell}(\boldsymbol{\Upsilon}\,\delta\boldsymbol{\phi})^{T}\boldsymbol{H}^{T}\,\boldsymbol{\mathcal{D}}\,\boldsymbol{H}\,(\boldsymbol{\Upsilon}\,\Delta\boldsymbol{\phi})\,dx. \tag{53}$$

To proceed with the formulation of the geometric stiffness terms we need first to linearize the virtual generalized strain measures in (39). This linearization gives:

$$\Delta\delta\boldsymbol{\varepsilon}=\begin{bmatrix}\delta\boldsymbol{u}'\cdot\Delta\boldsymbol{u}'\\ \delta\boldsymbol{u}'\cdot\Delta\boldsymbol{e}_3'+\delta\boldsymbol{e}_3'\cdot\Delta\boldsymbol{u}'+\boldsymbol{x}_0'\cdot\Delta\delta\boldsymbol{e}_3'\\ \delta\boldsymbol{u}'\cdot\Delta\boldsymbol{e}_2'+\delta\boldsymbol{e}_2'\cdot\Delta\boldsymbol{u}'+\boldsymbol{x}_0'\cdot\Delta\delta\boldsymbol{e}_2'\\ \delta\boldsymbol{u}'\cdot\Delta\boldsymbol{e}_2+\delta\boldsymbol{e}_2\cdot\Delta\boldsymbol{u}'+\boldsymbol{x}_0'\cdot\Delta\delta\boldsymbol{e}_2\\ \delta\boldsymbol{u}'\cdot\Delta\boldsymbol{e}_3+\delta\boldsymbol{e}_3\cdot\Delta\boldsymbol{u}'+\boldsymbol{x}_0'\cdot\Delta\delta\boldsymbol{e}_3\\ \delta\boldsymbol{e}_2'\cdot\Delta\boldsymbol{e}_3+\delta\boldsymbol{e}_3\cdot\Delta\boldsymbol{e}_2'+\boldsymbol{e}_3\cdot\Delta\delta\boldsymbol{e}_2'+\boldsymbol{e}_2'\cdot\Delta\delta\boldsymbol{e}_3\\ 2\left(\boldsymbol{e}_2'\cdot\Delta\delta\boldsymbol{e}_2'+\delta\boldsymbol{e}_2'\cdot\Delta\boldsymbol{e}_2'\right)\\ 2\left(\boldsymbol{e}_3'\cdot\Delta\delta\boldsymbol{e}_3'+\delta\boldsymbol{e}_3'\cdot\Delta\boldsymbol{e}_3'\right)\\ \delta\boldsymbol{e}_2'\cdot\Delta\boldsymbol{e}_3'+\delta\boldsymbol{e}_3'\cdot\Delta\boldsymbol{e}_2'+\boldsymbol{e}_3'\cdot\Delta\delta\boldsymbol{e}_2'+\boldsymbol{e}_2'\cdot\Delta\delta\boldsymbol{e}_3'\end{bmatrix}. \tag{54}$$

Then, the general expression of the geometrical tangent stiffness operator gives:

$$D_2\,G_{int}(\boldsymbol{\phi},\delta\boldsymbol{\phi})\cdot\Delta\boldsymbol{\phi}=\int_{\ell}\Delta\delta\boldsymbol{\varepsilon}^{T}\boldsymbol{S}\,dx. \tag{55}$$

Replacing (54) into (55), recalling the expressions of the incremental virtual directors $\Delta\delta\boldsymbol{e}_i$ (see A.2) and re arranging some terms, we can write the geometric stiffness operator as:

$$D_2\,G_{int}(\boldsymbol{\phi},\delta\boldsymbol{\phi})\cdot\Delta\boldsymbol{\phi}=\int_{\ell}(\boldsymbol{L}\,\delta\boldsymbol{\phi})^{T}\boldsymbol{G}\,(\boldsymbol{L}\,\Delta\boldsymbol{\phi})\,dx, \tag{56}$$

where the matrix $\boldsymbol{G}$ is given in A.3.

Since the external loads are assumed to be conservative, the linearization of the external virtual work is zero. As has been mentioned several times in geometrically exact formulations, a parametrization using spin variables necessarily implies a non conservative concentrated moment as its work conjugate variable. Indeed, it is well known the fact that the use of spin variables leads to a non-symmetric tangent stiffness matrix.

Finally, recalling (53) and (56) the linearized virtual work can be written as:

$$DG(\boldsymbol{\phi},\delta\boldsymbol{\phi})\cdot\Delta\boldsymbol{\phi}=\int_{\ell}(\boldsymbol{L}\,\delta\boldsymbol{\phi})^{T}(\boldsymbol{H}^{T}\,\boldsymbol{\mathcal{D}}\,\boldsymbol{H}+\boldsymbol{G})\,(\boldsymbol{L}\,\Delta\boldsymbol{\phi})\,dx. \tag{57}$$

6 FINITE ELEMENT FORMULATION

The implementation of the proposed finite element is based on linear interpolation and one point reduced integration. This approach relies on the interpolation of *iterative spin variables*.

6.1 Interpolation

Being $\boldsymbol{N_n}$ linear Lagrangean shape functions, we interpolate the position vectors in the undeformed and deformed configuration as (Zienkiewicz, 2000):

$$\widehat{\boldsymbol{X}} = \sum_{n=1}^{nxel} \boldsymbol{N_n}\, \boldsymbol{X_n}, \qquad \widehat{\boldsymbol{x}} = \sum_{n=1}^{nxel} \boldsymbol{N}_n \,(\boldsymbol{X}_n + \boldsymbol{u}_n), \tag{58}$$

where $nxel$ represent the number of nodes in the element. The same finite element interpolation is also applied to the configuration and the variations of the configuration.

6.2 Tangent Stiffness Matrix

In order to formulate the tangent stiffness matrix, we first recall the definition of the differential operator $\boldsymbol{\Upsilon}$ (see (41)). Using the interpolation function presented above, the differential operator $\boldsymbol{\Upsilon}$ can be replaced by its numeric counterpart in such a way that:

$$\boldsymbol{\Upsilon}\, \delta\boldsymbol{\phi} \cong \sum_{n=1}^{nxel} \boldsymbol{B}_n\, \delta\widehat{\boldsymbol{\phi}}_n, \tag{59}$$

where the matrix operator $\boldsymbol{B}_n$ contains shape functions and its derivatives and plays a crucial role in the finite element formulation. In the expressions presented hereafter, summation over index n will be implicitly defined. So:

$$\boldsymbol{B} = \begin{bmatrix} \boldsymbol{N'1} & \boldsymbol{0} \\ \boldsymbol{0} & \boldsymbol{N1} \\ \boldsymbol{0} & \boldsymbol{N'1} \end{bmatrix}. \tag{60}$$

Introducing (59) into (53) and (56) we can obtain the expressions for the material and geometric stiffness matrices respectively. Following this process we obtain first:

$$D_1 G_{int}\big(\widehat{\boldsymbol{\phi}}, \delta\widehat{\boldsymbol{\phi}}\big) \cdot \Delta\widehat{\boldsymbol{\phi}} = \int_\ell \big(\boldsymbol{B}\, \delta\widehat{\boldsymbol{\phi}}\big)^T \boldsymbol{H}^T\, \boldsymbol{\mathcal{D}}\, \boldsymbol{H}\, \big(\boldsymbol{B}\, \Delta\widehat{\boldsymbol{\phi}}\big)\, dx. \tag{61}$$

Proceeding in a similar way, the geometric stiffness term can be written as:

$$D_2 G_{int}\big(\widehat{\boldsymbol{\phi}}, \delta\widehat{\boldsymbol{\phi}}\big) \cdot \Delta\widehat{\boldsymbol{\phi}} = \int_\ell \big(\boldsymbol{B}\, \delta\widehat{\boldsymbol{\phi}}\big)^T \boldsymbol{G}\, \big(\boldsymbol{B}\, \Delta\widehat{\boldsymbol{\phi}}\big)\, dx. \tag{62}$$

Thus, the element materials and geometric stiffness matrices become:

$$\boldsymbol{k}_M = \int_\ell \boldsymbol{B}^T \boldsymbol{H}^T\, \boldsymbol{\mathcal{D}}\, \boldsymbol{H}\, \boldsymbol{B}\, dx, \qquad \boldsymbol{k}_G = \int_\ell \boldsymbol{B}^T \boldsymbol{G}\, \boldsymbol{B}\, dx. \tag{63}$$

Following the common steps of the finite element assembly process, the global tangent stiffness matrix is:

$$\boldsymbol{K}_T = \sum_{e=1}^{els} (\boldsymbol{k}_M + \boldsymbol{k}_G). \tag{64}$$

With an abuse in notation, the summation operator was used to represent the conventional finite element assembly operation.

6.3 Directors Update Algorithm

As already mentioned, the procedure used for updating the directors and its derivatives is iterative. This is, the current configuration is updated in each iteration. Being *n* the iteration counter we can recall (1) to find the new director as:

$$\boldsymbol{e}_i^{n+1} = \boldsymbol{\Lambda}\, \boldsymbol{e}_i^n, \tag{65}$$

where $\boldsymbol{\Lambda}$ is now the *incremental iterative rotation tensor*. Note that, although the formulation is based on the iterative spins, the director triads are "total rotation quantities". Note that the reference configuration is never updated, consequently only at the first iteration of the first increment we have $\boldsymbol{e}_i^1 = \boldsymbol{E}_i$:

According to (65), we can find the derivative of the directors as:

$$\boldsymbol{e}_i'^{\,n+1} = \boldsymbol{\Lambda}'\, \boldsymbol{e}_i^n + \boldsymbol{\Lambda}\, \boldsymbol{e}_i'^{\,n} = \boldsymbol{\Lambda}'\, \boldsymbol{\Lambda}^{\mathrm{T}}\, \boldsymbol{e}_i^{n+1} + \boldsymbol{\Lambda}\, \boldsymbol{e}_i'^{\,n}, \tag{66}$$

where the expression for the derivative of the rotation tensor (actually $\boldsymbol{\Lambda}'\boldsymbol{\Lambda}^{\mathrm{T}}$) can be found in A.4. Note that, in contrast to most multiplicative update algorithms, the evaluation of a total rotation tensor is never needed.

7 NUMERICAL INVESTIGATIONS

To close the development of the presented beam formulation we compare the performance of the proposed finite element with existing finite elements. We investigate both isotropic and tanisotropic beams, using some benchmark tests proposed in the literature.

It must be noted that since most of the reported benchmark tests were performed using solid cross sections, often it is not possible to find an equivalent thin-walled section with the same mass and inertia properties to those of the solid sections. Because of that, we have used the research finite element software FEAP (Taylor, 2009) to obtain results using the Simo and Vu-Quoc (1986) and Ibrahimbegovic (1997) finite elements (which are included in the package). In these calculations we have used cross sections with the same inertia moments of the thin-walled cross section.

In the analysis of anisotropic beams we have chosen to compare the present formulation exclusively against Abaqus 3D shell models, thus having the possibility of handling any type of laminate.

7.1 Pure bending of a cantilever isotropic beam

To validate the formulation and especially the finite rotation algorithm we compare our beam model using an isotropic constitutive law against the classical Simo and Vu-Quoc (1986) beam model. We choose the roll-up test to perform this comparison. We choose a thin-walled beam with a square cross section ($b = 0.5$, $h = 0.5$ and $t = 0.05$) and a length of 50. The material constants are: $E=144\times10^9$ and $\nu=0.3$. Being the Euler formula:

$$\theta = \frac{M\, l}{E\, I} \tag{67}$$

We can obtain the magnitude of the moment that produces a deformed shape of half a circle or full circle. To obtain these deformed shapes we must apply moments $M_1=3.80761\times10^7$ and $M_2=7.615221\times10^7$. Figure 3 shows the deformed shapes obtained after application of these moments.

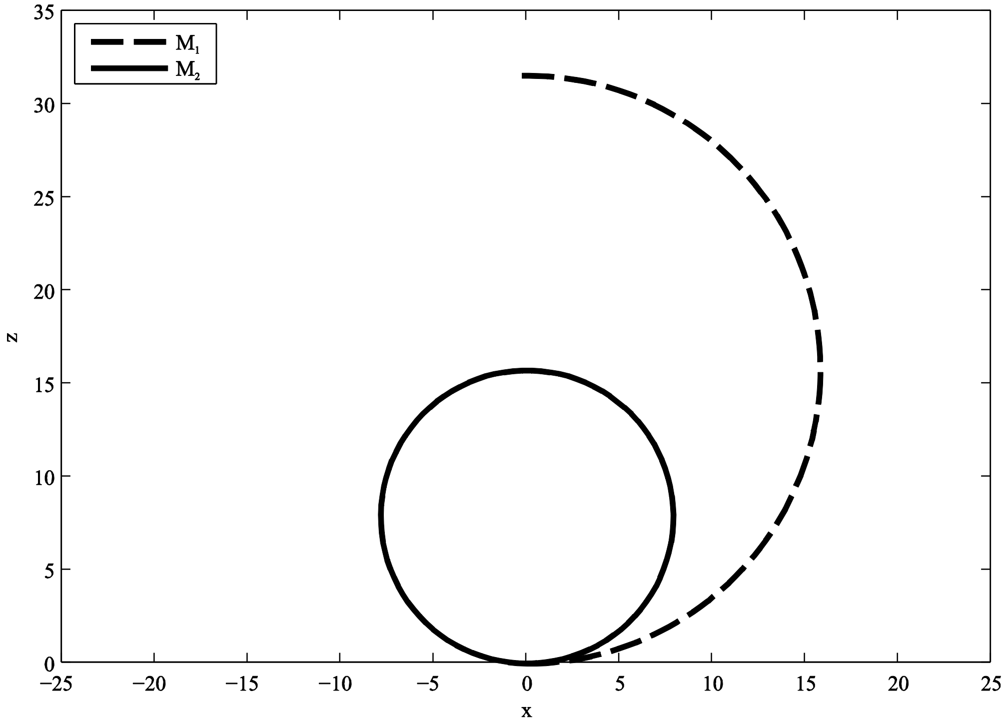

Figure 3 – Roll up test.

Tables 1 and 2 present the numerical results obtained for the maximum tip displacements for both load cases (M_1 and M_2)

	Tip Vertical Displacement	Tip Horizontal Displacement	Max Vertical Displacement	Elements
Simo & Vu-Quoc (FEAP)	31.673	-50.448	31.673	10
Ibrahimbegovic (FEAP)	31.673	-50.448	31.673	10
Analytic	31.831	-50.000	31.831	-
Present	31.694	-50.405	31.694	10

Table 1 – Displacements Components for M_1.

As it can be seen from the tables, the performance of the presented finite element is very good. Both the vertical and horizontal displacements agree very well with the results obtained using the well validated Simo and Vu-Quoc model (1986).

	Tip Vertical Displacement	Tip Horizontal Displacement	Max Vertical Displacement	Elements
Simo & Vu-Quoc (FEAP)	0.013	-49.545	16.038	10
Analytic	0.000	-50.000	15.915	-

Present	0.016	-49.494	16.004	10

Table 2 – Displacements Components for M_2.

The differences between the Simo and Vu-Quoc model and the proposed model are originated due to the different hypotheses introduced in both models. The proposed model allows thickness shear deformation while the model in (Simo and Vu-Quoc, 1986) (and also (Ibrahimbegovic, 1997)) doesn't. Also, the inertia moments resulting from the present formulation are slightly lower than those that feed a Timoshenko model; this difference makes the present model to be slightly more flexible than a traditional beam model.

7.2 Pure bending of a cantilever beam

To test the performance of the presented finite element in a full three dimensional problem we study the behavior of a curved cantilever beam (see. Fig. 5). The curved beam has a reference configuration given as a 45º circular segment with radius $R=100$ and laying in the x-y plane, the beam is loaded with a vertical load (z direction). The properties of the isotropic material are: $E=1.0\times10^7$ and $\nu=0.3$. The cross section is a box with $b=1$, $h=1$ and $t=0.1$.

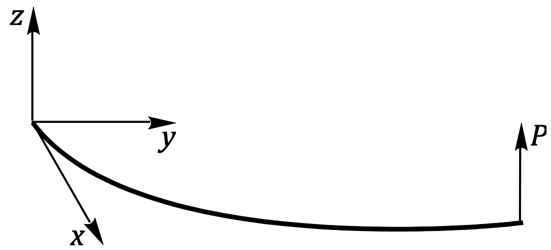

Figure 4 – 45º arc bending

Table 3 shows the results of the bending test for $P=400$. We have used an Abaqus 3D shell model as the reference model. As it can be seen, the present finite element formulation behaves very well compared to the Simo & Vu-Quoc element available in FEAP and also to the Abaqus B31 and B32 beam elements.

	Tip y Displacement	Tip x Displacement	Max z Displacement	Elements
Abaqus Shell	-12.201	-21.546	50.997	-
Abaqus B31	-12.401	-21.311	-51.110	50
Abaqus B32	-12.416	-21.310	-51.111	50
Simo & Vu-Quoc (FEAP)	-12.008	-20.692	50.067	50
Present	-12.205	-21.015	50.880	50

Table 3 – Maximum displacements in a 45º arc bending test (*P=400*)

Taking as a reference the Abaqus shell model, the percentile error of the present model is about 0.25% this is well below the 1.8 % error obtained with the Simo and Vu-Quoc element.

In order to study the behavior of the proposed finite element when using anisotropic laminates, we analyze the 45º arc of Fig. 5 laminated with a {45,-45,-45,45} configuration. The laminas are made of E-Glass fibers and an Epoxy matrix, the material properties are:

E_{11}	E_{22}	G_{12}	G_{23}	ν_{12}
45.0×10^9	12.0×10^9	5.5×10^9	5.5×10^9	0.3

Table 4 – Material properties of E-Glass Fiber-Epoxy lamina.

To increase the complexity of the stress state in the beam we modify the applied load to have components $P_x=4.0\times10^5$, $P_y=-4.0\times10^5$, $P_z=8.0\times10^5$. Figure 6 presents the curves that describe the evolution of the displacements along the load path.

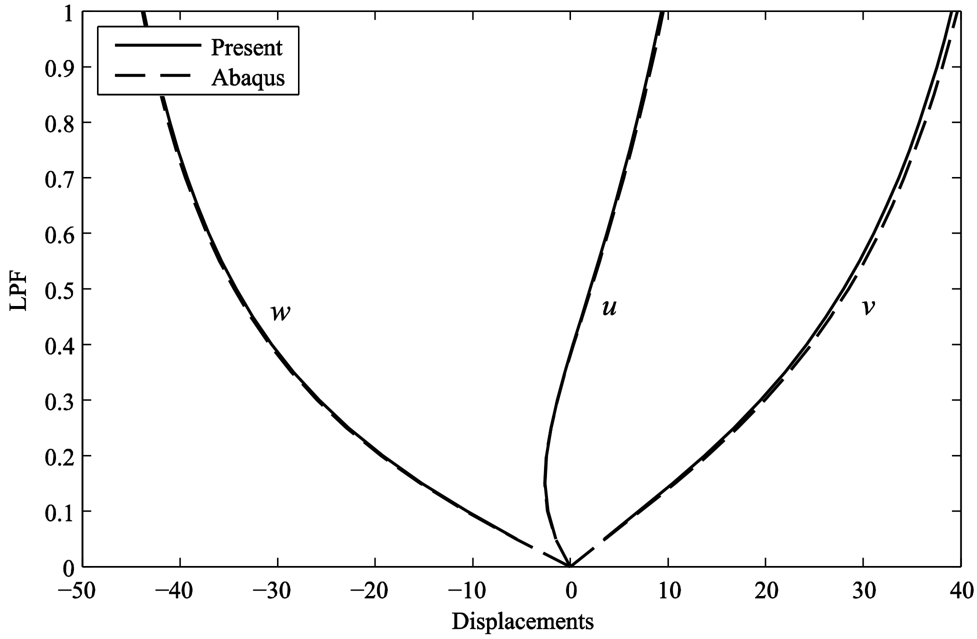

Figure 5. Displacement components vs. Load Proportional Factor – 45º anisotropic arc.

It can be seen from Fig. 5 that the correlation of the present formulation against the Abaqus shell model is excellent, note that this good correlation does not deteriorate when the displacements grow.

7.4 Post buckling of curved arc – Limit Point traversal.

The problem of traversal of limit points has been used several times as a benchmark test for geometrical nonlinear theories of isotropic beams, see e.g. (Ibrahimbegovic, 1995). We analyze the behavior a curved thin-walled arc (see Figure 6), as shown in Fig. 6, for both isotropic and anisotropic materials. The arc cross section is box with $b=1$, $h=1$ and $t=0.1$.

Although the arc buckles, the buckling phenomenon studied in this example is not characterized by a bifurcation in the nonlinear phase-plane but by a limit point traversal. A vertical load creates a compressive stress state that causes the buckling of the arc. The load displacement path was followed using the arc-length method.

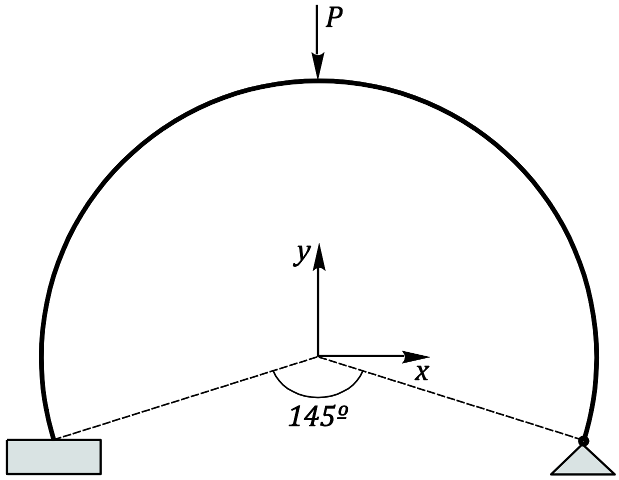

Figure 6. 215º Thin-walled arc

In Figure 7 the load-displacement curve of the isotropic arc using the present formulation is compared vs. the Simo and Vu-Quoc element implemented in FEAP and an Abaqus shell model. The isotropic material properties are: $E=144\times10^{9}$ and $\nu=0.3$. It can be observed that the present formulation gives very good results even for extremely large displacements. It can also be observed that the present formulation is slightly more flexible than the Simo and Vu-Quoc finite element. Also, and as expected, the 3D shell model is more flexible that both beam formulations. This fact is ascribed mainly to the deformability of the cross section.

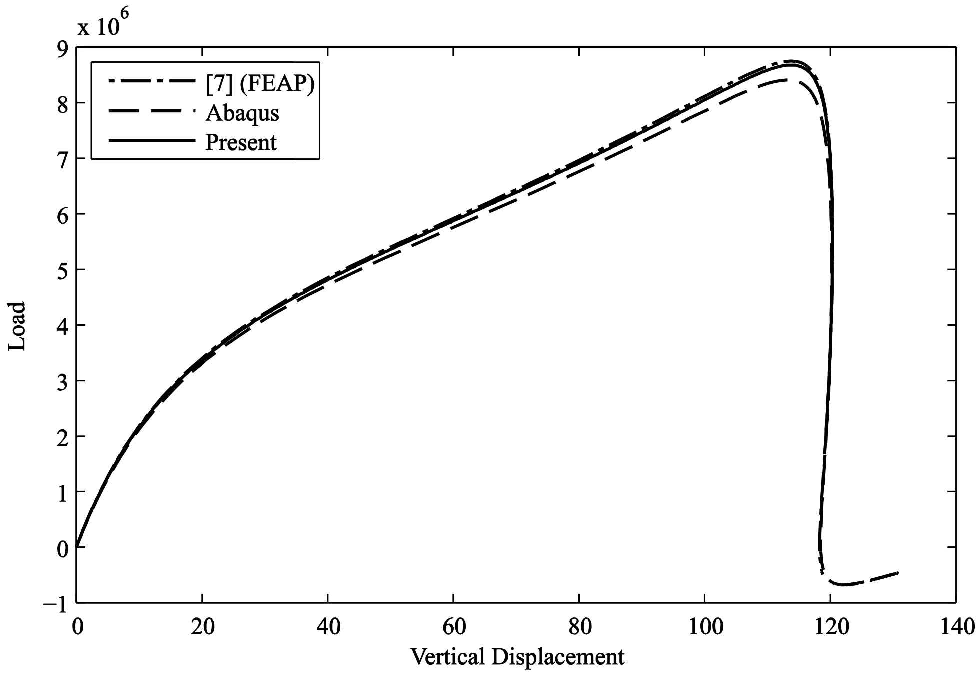

Figure 7 – Load-Displacement curve for isotropic (E=144E9)

Figure 8 shows the deformed shape of the structure after the critical point has been traversed.

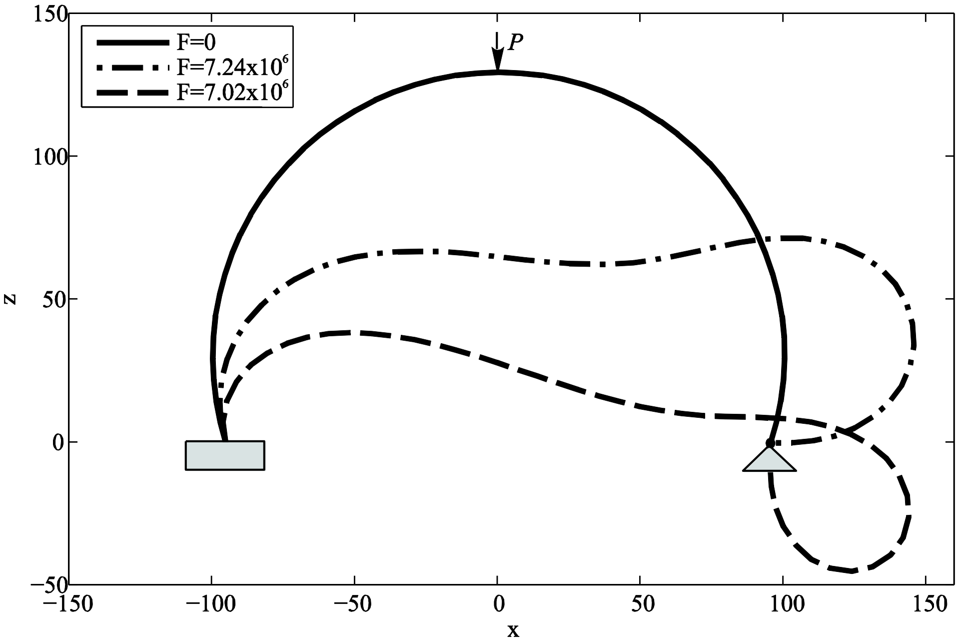

Figure 8 – Deformed shape (isotropic arc)

Figure 9 shows the load-displacement relation during the collapse of the composite arc. We compare the present model with an Abaqus 3D shell model. In this example we have used a cross section laminated with 4 layers of E-Glass fibers and an Epoxy matrix, oriented in directions {0,90,90,0}.

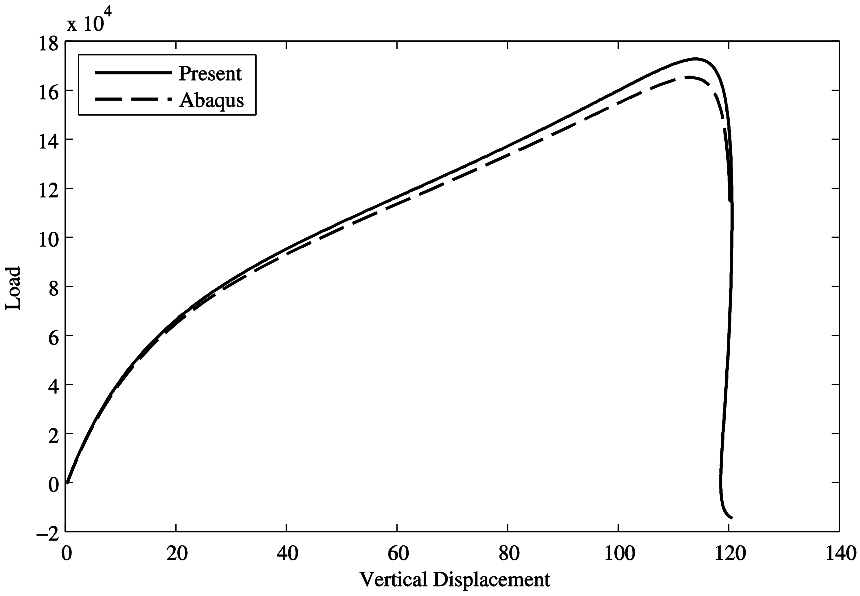

Figure 9 – Load-Displacement curve for {0,90,90,0} E-FiberGlass-Epoxi

8 CONCLUSIONS

An Eulerian geometrically exact beam finite element for composite thin-walled beams has been presented. The proposed formulation relies on the parametrization of the weak form of equilibrium in terms of the director field and its derivatives. Spatial spins were used to establish the relationship between the director field and the configuration, and a new iterative update procedure for the director triad was proposed. Also, a method to embed the thin-walled beam theory into any existing finite rotation algorithm was presented.

The evaluation of the weak form of equilibrium was aided by the introduction of generalized strains, resulting from a dual transformation of the rectangular GL strains. The generalized strains work conjugate variables, i.e. the generalized beam forces, were deduced from the curvilinear shell stresses before the obtention of the weak form.

Representative numerical experiments show that the presented thin-walled beam formulation has an excellent correlation against existing finite elements for isotropic materials. For the case of composite materials, the correlation against superior theories such as 3D shell models was also excellent.

The possibility of using any type of composite material represents an important advantage of the present formulation over existing displacement based geometrically exact finite element beam formulations. The accounting of all existing geometrical and material couplings regardless of the magnitude of displacements and rotations is an important achievement of the present formulation.

9 ACKNOWLEDGEMENTS

The authors wish to acknowledge the supports from Secretaría de Ciencia y Tecnología of Universidad Tecnológica Nacional, Departamento de Ingeniería of Universidad Nacional del Sur and CONICET.

APPENDIX A

A.1 Matrix $\widehat{\boldsymbol{D}}$

Introducing (18) into the matrix $\widehat{\boldsymbol{D}}$ we can obtain a cross sectional matrix as a function of the midsurface coordinates, this is:

$$\widehat{\boldsymbol{D}} = \begin{bmatrix} 1 & n\,\bar{\xi}_2' + \bar{\xi}_3 & -n\,\bar{\xi}_3' + \bar{\xi}_2 & 0 & 0 & 0 & 0 & 0 & a_1 & a_2 & a_3 \\ 0 & 0 & 0 & \bar{\xi}_2' & \bar{\xi}_3' & b_1 & -n\,\bar{\xi}_2'\bar{\xi}_3' + \bar{\xi}_2\bar{\xi}_2' & n\,\bar{\xi}_2'\bar{\xi}_3' + \bar{\xi}_3\bar{\xi}_3' & 0 & 0 & 0 \\ 0 & 0 & 0 & -\bar{\xi}_3' & \bar{\xi}_2' & \bar{\xi}_2\bar{\xi}_2' + \bar{\xi}_3\bar{\xi}_3' & n\,\bar{\xi}_3'^{\,2} - \bar{\xi}_2\bar{\xi}_3' & n\,\bar{\xi}_2'^{\,2} + \bar{\xi}_3\bar{\xi}_2' & 0 & 0 & 0 \end{bmatrix}, \tag{A1}$$

where the coefficients a_i and b_i are:

$$\begin{aligned} a_1 &= \frac{1}{2}n^2\bar{\xi}_3'^{\,2} - n\bar{\xi}_3'\bar{\xi}_2 + \frac{\bar{\xi}_2^{\,2}}{2}, \\ a_2 &= \frac{1}{2}n^2\bar{\xi}_2'^{\,2} + n\bar{\xi}_2'\bar{\xi}_3 + \frac{\bar{\xi}_3^{\,2}}{2}, \\ a_3 &= -n^2\bar{\xi}_2'\bar{\xi}_3' + \bar{\xi}_2\bar{\xi}_3 + n(\bar{\xi}_2'\bar{\xi}_2 - \bar{\xi}_3', \\ b_1 &= -n\left(\bar{\xi}_2'^{\,2} + \bar{\xi}_3'^{\,2}\right) + \left(\bar{\xi}_2\bar{\xi}_3' - \bar{\xi}_3\bar{\xi}_2'\right). \end{aligned} \tag{A2}$$

Explicitly the beam forces vector gives:

$$\begin{bmatrix} N \\ M_2 \\ M_3 \\ Q_2 \\ Q_3 \\ T \\ P_2 \\ P_3 \\ P_{23} \end{bmatrix} = \begin{pmatrix} N_{xx} \\ M_{xx}\,\bar{\xi}_2' + N_{xx}\,\bar{\xi}_3 \\ -M_{xx}\,\bar{\xi}_3' + N_{xx}\,\bar{\xi}_2 \\ N_{xs}\,\bar{\xi}_2' - N_{xn}\,\bar{\xi}_3' \\ N_{xn}\,\bar{\xi}_2' + N_{xs}\,\bar{\xi}_3' \\ -M_{xs}\left(\bar{\xi}_2'^{\,2} + \bar{\xi}_3'^{\,2}\right) + N_{xs}\left(\bar{\xi}_3'\bar{\xi}_2 - \bar{\xi}_2'\bar{\xi}_3\right) + N_{xn}\left(\bar{\xi}_2'\bar{\xi}_2 + \bar{\xi}_3'\bar{\xi}_3\right) \\ -M_{xx}\,\bar{\xi}_3'\,\bar{\xi}_2 + \dfrac{1}{2}N_{xx}\,\bar{\xi}_2^{\,2} \\ M_{xx}\,\bar{\xi}_2'\,\bar{\xi}_3 + \dfrac{1}{2}N_{xx}\,\bar{\xi}_3^{\,2} \\ N_{xx}\,\bar{\xi}_2\,\bar{\xi}_3 + M_{xx}\left(\bar{\xi}_2'\bar{\xi}_2 - \bar{\xi}_3'\bar{\xi}_3\right) \end{pmatrix}. \tag{A3}$$

A.2 Second Variation of directors

The second variation of the director field is obtained in a standard manner. For the sake of brevity we show only how to obtain the second variation of the derivative of the director field. Being $\boldsymbol{b}$ any vector, we can obtain the second variation of the director's derivative as:

$$\begin{aligned} \boldsymbol{b}\cdot\Delta\delta\boldsymbol{e}_3' &= \boldsymbol{b}\cdot\Delta(\delta\boldsymbol{w}'\times\boldsymbol{e}_i) + \boldsymbol{b}\cdot\Delta\left(\delta\boldsymbol{w}\times\boldsymbol{e}_i'\right) \\ &= \boldsymbol{b}\cdot\left(\delta\boldsymbol{w}'\times(\Delta\boldsymbol{w}\times\boldsymbol{e}_i)\right) + \boldsymbol{b}\cdot\left(\delta\boldsymbol{w}\times(\Delta\boldsymbol{w}'\times\boldsymbol{e}_i + \Delta\boldsymbol{w}\times\boldsymbol{e}_i')\right) \\ &= \boldsymbol{b}\cdot\left(\delta\boldsymbol{w}'\times(\Delta\boldsymbol{w}\times\boldsymbol{e}_i)\right) + (\boldsymbol{b}\times\delta\boldsymbol{w})\cdot(\Delta\boldsymbol{w}'\times\boldsymbol{e}_i) + (\boldsymbol{b}\times\delta\boldsymbol{w}) \\ &\quad\cdot(\Delta\boldsymbol{w}\times\boldsymbol{e}_i') \\ &= \delta\boldsymbol{w}'\left[\tilde{\boldsymbol{b}}\,\tilde{\boldsymbol{e}}_i\right]\Delta\boldsymbol{w} + \delta\boldsymbol{w}\left[\tilde{\boldsymbol{b}}\,\tilde{\boldsymbol{e}}_i\right]\Delta\boldsymbol{w}' + \delta\boldsymbol{w}\left[\tilde{\boldsymbol{b}}\,\tilde{\boldsymbol{e}}_i'\right]\Delta\boldsymbol{w} \end{aligned} \tag{A4}$$

Where $\tilde{\ }$ denotes the skew symmetric matrix of vector as defined in (35). Proceeding in a similar way we can obtain all the second variations.

A.3 Matrix $\boldsymbol{G}$

The full expression of the geometric matrix $\boldsymbol{G}$ gives:

$$\boldsymbol{G} = \begin{bmatrix} N & -(M_2\boldsymbol{e}_3' + M_3\boldsymbol{e}_2') - (Q_2\boldsymbol{e}_2 + Q_3\boldsymbol{e}_3) & -(M_2\boldsymbol{e}_3 + M_3\boldsymbol{e}_2) \\ M_2\boldsymbol{e}_3' + M_3\boldsymbol{e}_2' + Q_2\boldsymbol{e}_2 + Q_3\boldsymbol{e}_3 & M_2\boldsymbol{x}_0'\boldsymbol{e}_3' + M_3\boldsymbol{x}_0'\boldsymbol{e}_2' + Q_2\boldsymbol{x}_0'\boldsymbol{e}_2 + Q_3\boldsymbol{x}_0'\boldsymbol{e}_3 & M_2\boldsymbol{x}_0'\boldsymbol{e}_3 + M_3\boldsymbol{x}_0'\boldsymbol{e}_2 \\ M_2\boldsymbol{e}_3 + M_3\boldsymbol{e}_2 & M_2\boldsymbol{x}_0'\boldsymbol{e}_3 + M_3\boldsymbol{x}_0'\boldsymbol{e}_2 + \boldsymbol{G}_{23} & \boldsymbol{G}_{33} \end{bmatrix} \tag{A5}$$

Where the $\boldsymbol{G}_{ij}$ coefficients are:

$$\begin{aligned} \boldsymbol{G}_{23} &= -T\boldsymbol{e}_1 + 2\left[P_2\left(\overline{\boldsymbol{e}_2'\boldsymbol{e}_2} + \overline{\boldsymbol{e}_2 - \boldsymbol{e}_2'}\right) + P_3\left(\overline{\boldsymbol{e}_3'\boldsymbol{e}_3} + \overline{\boldsymbol{e}_3 - \boldsymbol{e}_3'}\right)\right] \\ &\qquad + P_{23}\left[\left(\overline{\boldsymbol{e}_2'\boldsymbol{e}_3} + \overline{\boldsymbol{e}_3'\boldsymbol{e}_2}\right) + \left(\overline{\boldsymbol{e}_3 - \boldsymbol{e}_2'} + \overline{\boldsymbol{e}_2 - \boldsymbol{e}_3'}\right)\right] \\ \boldsymbol{G}_{33} &= 2P_2\,\overline{\boldsymbol{e}_2 - \boldsymbol{e}_2} + 2P_3\,\overline{\boldsymbol{e}_3 - \boldsymbol{e}_3} + P_{23}\,\left[\overline{\boldsymbol{e}_3 - \boldsymbol{e}_2} + P_3\,\overline{\boldsymbol{e}_2 - \boldsymbol{e}_3}\right] \end{aligned} \tag{A6}$$

A.4 Derivative of the Exponential Map

An alternative expression for (6) can be written as:

$$\boldsymbol{\Lambda} = \boldsymbol{I} + \frac{2}{1 + \left\|\bar{\boldsymbol{\vartheta}}\right\|^2}\left(\bar{\boldsymbol{\Theta}} + \bar{\boldsymbol{\Theta}}^2\right), \tag{A7}$$

Where $\bar{\boldsymbol{\vartheta}}$ is a scaled pseudo-vector such that:

$$\bar{\boldsymbol{\vartheta}} = tan\left(\tfrac{1}{2}\|\Delta \boldsymbol{w}\|\right)\boldsymbol{t}, \quad \boldsymbol{t} = \frac{\Delta \boldsymbol{w}}{\|\Delta \boldsymbol{w}\|} \tag{A8}$$

and $\bar{\boldsymbol{\Theta}}$ is the skew symmetric matrix of $\bar{\boldsymbol{\vartheta}}$. Derivating with respect to x we have:

$$\boldsymbol{\Lambda}' = \frac{2}{1+\|\bar{\boldsymbol{\vartheta}}\|^2}\left[\bar{\boldsymbol{\Theta}}' + \bar{\boldsymbol{\Theta}}'\,\bar{\boldsymbol{\Theta}} + \bar{\boldsymbol{\Theta}}\,\bar{\boldsymbol{\Theta}}' - \frac{2\bar{\boldsymbol{\vartheta}}\cdot\bar{\boldsymbol{\vartheta}}'(\bar{\boldsymbol{\Theta}} + \bar{\boldsymbol{\Theta}}^2)}{1+\|\bar{\boldsymbol{\vartheta}}\|^2}\right], \tag{A9}$$

After some manipulations and identities it can be found that:

$$\boldsymbol{\Lambda}'\boldsymbol{\Lambda}^T = \frac{2}{1+\|\bar{\boldsymbol{\vartheta}}\|^2}(\bar{\boldsymbol{\Theta}}' - \bar{\boldsymbol{\Theta}}'\,\bar{\boldsymbol{\Theta}} + \bar{\boldsymbol{\Theta}}\,\bar{\boldsymbol{\Theta}}') \tag{A10}$$

Recalling (66) we see that obtaining a close expression for $\boldsymbol{\Lambda}'\boldsymbol{\Lambda}^T$ we can update the derivatives of the directors without the necessity of obtaining a close expression for $\boldsymbol{\Lambda}'$. Therefore, the above expression is used in (66).

REFERENCES

ANTMAN, S. S. 1976. Ordinary differential equations of one dimensional elasticity: foundations of the theories of nonlinearly elastic rods and shells. *Arch. Rational Mech,* 61.

ARGYRIS, J. 1982. An excursion into large rotations. *Computer Methods in Applied Mechanics and Engineering,* 32**,** 85-155.

ARMERO, F. & ROMERO, I. 2001. On the objective and conserving integration of geometrically exact rod models. *In:* WALL, W. A., BLETZINGER, K. U. & SCHWEIZERHOF, K. (eds.) *Trends in computational structural mechanics.* Barcelona, Spain: CIMNE.

BARBERO, E. 2008. *Introduction to Composite Material Design,* London, Taylor and Francis.

BATHE, K.-J. & BOLOURCHI, S. 1979. Large displacement analysis of three-dimensional beam structures. *International Journal for Numerical Methods in Engineering,* 14**,** 961-986.

BETSCH, P. & STEINMANN, P. 2002. Frame-indifferent beam finite elements based upon the geometrically exact beam theory. *International Journal for Numerical Methods in Engineering,* 54**,** 1775-1788.

BONET, J. W., R.D. 1997. *Nonlinear Continuum Mechanics for Finite Element Analysis,* Cambridge, Cambridge University Press.

CARDONA, A. & GERADIN, M. 1988. A beam finite element non-linear theory with finite rotations. *International Journal for Numerical Methods in Engineering,* 26**,** 2403-2438.

CRISFIELD, M. A. 1997. *Non-Linear Finite Element Analysis of Solids and Structures: Advanced Topics*, John Wiley \& Sons, Inc.

GRUTTMANN, F., SAUER, R. & WAGNER, W. 1998. A geometrical nonlinear eccentric 3D-beam element with arbitrary cross-sections. *Computer Methods in Applied Mechanics and Engineering,* 160**,** 383-400.

HODGES, D. H., YU, W. & PATIL, M. J. 2009. Geometrically-exact, intrinsic theory for dynamics of moving composite plates. *International Journal of Solids and Structures,* 46**,** 2036-2042.

IBRAHIMBEGOVIC, A. 1995. On finite element implementation of geometrically nonlinear Reissner's beam theory: three-dimensional curved beam elements. *Computer Methods in Applied Mechanics and Engineering,* 122**,** 11-26.

IBRAHIMBEGOVIC, A. 1997. On the choice of finite rotation parameters. *Computer Methods in Applied Mechanics and Engineering,* 149**,** 49-71.

JONES, R. M. 1999. *Mechanics of Composite Materials,* London, Taylor & Francis.

LIBRESCU, L. 2006. *Thin-Walled Composite Beams,* Dordrecht, Springer.

MACHADO, S. P. & CORTÍNEZ, V. H. 2005. Non-linear model for stability of thin-walled composite beams with shear deformation. *Thin-Walled Structures,* 43**,** 1615-1645.

PIOVAN, M. T. & CORTÍNEZ, V. H. 2007. Mechanics of thin-walled curved beams made of composite materials, allowing for shear deformability. *Thin-Walled Structures,* 45**,** 759-789.

REISSNER, E. 1972. A one-dimensional finite strain beam theory: the plane problem. *Journal of Applied Mathematics and Physics,* 23**,** 307-351.

RITTO-CORRÊA, M. & CAMOTIM, D. 2003. Work-conjugacy between rotation-dependent moments and finite rotations. *International Journal of Solids and Structures,* 40**,** 2851-2873.

ROMERO, I. & ARMERO, F. 2002. An objective finite element approximation of the kinematics of geometrically exact rods and its use in the formulation of an energy-momentum conserving scheme in dynamics. *International Journal for Numerical Methods in Engineering,* 54**,** 1683–1716.

SIMO, J. C. 1985. A finite strain beam formulation. The three-dimensional dynamic problem. Part I. *Computer Methods in Applied Mechanics and Engineering,* 49**,** 55-70.

SIMO, J. C. & VU-QUOC, L. 1986. A three-dimensional finite-strain rod model. part II: Computational aspects. *Computer Methods in Applied Mechanics and Engineering,* 58**,** 79-116.

TAYLOR, R. 2009. FEAP Users Manual. *FEAP* Berkeley.

WASHIZU, K. 1968. *Variational Methods in Elasticity and Plasticity,* Oxford, Pergamon Press.

ZIEGLER, H. 1968. *Principles of Structural Stability,* Waltham, Massachusetts, Blaisdell Publishing Co.

ZIENKIEWICZ, O. C. 2000. *The Finite Element Method,* Oxford, Buttherworth-Heinemann.